Intelligent Geometric Dynamics: A Generative Architecture Based on Manifold Metrics and Geodesic Energy Flow

Ning HU Gemini 3 Pro Claude Opus 4.5

January 16, 2026

Abstract

We propose a novel theoretical framework for deep learning that fundamentally reconceptualizes intelligent generative processes through the lens of differential geometry and physical field theory. Our central hypothesis posits that the performance of intelligent systems emerges from structural energy flow, where information transmission follows geodesic paths on learned Riemannian manifolds. This represents a paradigm shift from traditional function approximation in Euclidean space to *manifold geometric evolution*. We introduce the **Riemannian Geodesic Transformer**, an architecture where training corresponds to metric tensor learning and inference manifests as geodesic navigation governed by the principle of least action. We develop mathematically rigorous formulations including gyroscopic attention mechanisms based on geodesic distance, Fréchet mean aggregation for curved spaces, and exponential map residual connections. Furthermore, we address critical engineering challenges through tangent space approximations, dimensionality reduction via hyperbolic embeddings, and custom kernel fusion strategies. Theoretical analysis and preliminary projections suggest that our optimized Riemannian architecture can achieve competitive computational efficiency (1.5-2× baseline latency) while offering superior parameter efficiency and enhanced logical reasoning capabilities, particularly for hierarchically structured data.

Keywords: Riemannian Geometry, Geodesic Flow, Transformer Architecture, Hyperbolic Embeddings, Differential Geometry, Geometric Deep Learning

1 Introduction

The remarkable success of deep learning over the past decade has been built predominantly upon architectures operating within Euclidean vector spaces. From convolutional neural networks to the transformer architecture that now dominates natural language processing and beyond, the fundamental computational substrate assumes that learned representations inhabit flat, Euclidean geometry. While this assumption has proven remarkably effective, it may represent a fundamental limitation when modeling phenomena with inherent geometric structure.

Consider the challenge of representing hierarchical relationships—taxonomies, organizational structures, or logical dependencies. In Euclidean space, embedding a tree with n nodes requires $\Omega(\sqrt{n})$ dimensions to achieve bounded distortion, a consequence of the polynomial volume growth of Euclidean balls. This dimensional requirement becomes prohibitive for large-scale hierarchies and suggests a fundamental mismatch between the geometry of the representation space and the structure being represented.

1.1 Motivation and Core Hypothesis

This work is motivated by a simple yet profound observation: *the geometry of the representation space should match the geometry of the data.* We propose that intelligent generative processes can be understood as manifestations of structural energy flow, where information transmission follows geodesic paths on appropriately curved manifolds.

> **Core Hypothesis:** The performance of the intelligent generative process is the manifestation of structural energy flow, where energy transmission follows geodesic paths on learned Riemannian manifolds.

This hypothesis suggests a fundamental reconceptualization of deep learning: rather than viewing neural networks as function approximators in Euclidean space, we propose viewing them as geometric structures that learn appropriate curvature to minimize the energy required for information flow.

1.2 Paradigm Shift

Our framework represents a paradigm shift along several dimensions:

1. **From Function Approximation to Geometric Evolution:** Traditional deep learning seeks to approximate unknown functions through composition of parameterized transformations. Our framework instead views learning as the evolution of a geometric structure—specifically, the metric tensor field that defines distances and angles on the representation manifold.

2. **From Algebraic to Geometric Computation:** Standard neural network operations (matrix multiplication, nonlinear activation) are fundamentally algebraic. We replace these with geometric operations: exponential maps, parallel transport, and geodesic integration.

3. **From Arbitrary Trajectories to Optimal Paths:** In traditional architectures, the path through representation space during inference is determined by arbitrary compositions of learned transformations. In our framework, inference follows geodesics—paths of minimal energy expenditure governed by the principle of least action.

1.3 Contributions

The main contributions of this paper are:

1. A rigorous theoretical framework connecting deep learning to differential geometry and physical field theory, establishing formal correspondences between training/inference and metric learning/geodesic navigation.

2. The **Riemannian Geodesic Transformer** architecture, featuring novel geometric analogs of attention mechanisms, residual connections, and feed-forward layers.

3. A comprehensive analysis of engineering challenges and optimization strategies for implementing Riemannian neural networks on modern GPU hardware.

4. A strategic framework for selecting appropriate manifold geometries (hyperbolic, spherical, Euclidean, or products thereof) based on data structure.

2 Related Work

2.1 Hyperbolic Neural Networks

The application of hyperbolic geometry to machine learning was pioneered by Nickel and Kiela [2017], who demonstrated that the Poincaré ball model could embed hierarchical structures with remarkably low distortion in low dimensions. This work sparked extensive research into hyperbolic neural networks.

Ganea et al. [2018] extended these ideas to develop hyperbolic neural network layers, introducing hyperbolic versions of feed-forward networks, attention mechanisms, and recurrent architectures. Their key insight was the use of Möbius gyrovector operations to generalize linear transformations to hyperbolic space.

More recently, Chami et al. [2019] proposed Hyperbolic Graph Convolutional Networks (HGCN), demonstrating superior performance on hierarchically structured graph data. Liu et al. [2019] introduced hyperbolic attention networks, and Chen et al. [2021] developed fully hyperbolic neural networks that operate entirely in hyperbolic space without tangent space projections.

2.2 Geometric Deep Learning

The broader field of geometric deep learning [Bronstein et al., 2021] provides a unifying framework for neural network architectures that respect geometric structure. This includes graph neural networks [Kipf and Welling, 2016, Veličković et al., 2018], equivariant networks [Cohen and Welling, 2016, Weiler et al., 2019], and manifold-valued networks [Huang and Van Gool, 2017].

Nickel and Kiela [2018] provided theoretical foundations for learning continuous hierarchies, while Sala et al. [2018] established fundamental limits on embedding quality in different geometric spaces.

2.3 Information Geometry and Natural Gradients

Information geometry [Amari, 2016] studies the geometric structure induced by probability distributions. The Fisher information metric defines a Riemannian structure on statistical manifolds, and natural gradient descent [Amari, 1998] exploits this structure for more efficient optimization.

Martens [2020] provided modern perspectives on natural gradient methods, while [Zhang et al., 2019] connected Riemannian optimization to deep learning.

2.4 Physics-Inspired Deep Learning

Several works have drawn inspiration from physics for neural network design. Hamiltonian Neural Networks [Greydanus et al., 2019] learn to respect conservation laws, while Neural ODEs [Chen et al., 2018] view residual networks as discretizations of continuous dynamical systems.

Our work differs from these approaches by focusing on the *geometric* rather than *dynamical* aspects of physics, viewing the learned metric tensor as encoding the structure of knowledge itself.

3 Theoretical Foundation: The Isomorphism of Physics and Geometry

Traditional deep learning treats intelligence as function fitting within high-dimensional Euclidean space. Our architecture is built upon a fundamentally different foundation: **differential geometry** and **physical field theory**. In this section, we establish the mathematical foundations and draw precise connections between geometric structures and intelligent computation.

3.1 Core Definitions

Definition 3.1 (Intelligence Manifold). *The **structure of intelligence** is modeled as a Riemannian manifold $(\mathcal{M}, g)$, where:*

- *$\mathcal{M}$ is a smooth manifold representing the topological space of all possible concepts, semantic states, or latent representations.*
- *$g = \{g_{ij}(x)\}$ is a smoothly varying positive-definite metric tensor field that defines the local geometry at each point $x \in \mathcal{M}$.*

The metric tensor g encodes what we call "knowledge"—it defines the semantic distance between concepts, the strength of associations, and the natural pathways for reasoning. Specifically:

Proposition 3.2 (Metric as Knowledge). *The learned metric tensor $g_{ij}(x)$ encodes:*

1. ***Semantic Distance:** The geodesic distance $d_{\mathcal{M}}(x, y)$ between points $x, y \in \mathcal{M}$ represents the semantic dissimilarity between corresponding concepts.*
2. ***Associative Strength:** High curvature regions correspond to dense semantic neighborhoods with strong inter-concept associations.*
3. ***Reasoning Pathways:** Geodesics represent optimal inferential paths requiring minimal cognitive "energy."*

Definition 3.3 (Generative Process as Geodesic Motion). *The **generative process** (inference) is defined as geodesic motion on $(\mathcal{M}, g)$. Given an initial state x_0 (corresponding to input/prompt), the system evolves along geodesics toward target states (corresponding to outputs/answers), governed by the **principle of least action**.*

3.2 Physical Interpretation

The connection to physics runs deep. In general relativity, massive objects curve spacetime, and free particles follow geodesics—paths of extremal proper time. In our framework:

- **Training** corresponds to learning the curvature of conceptual space, analogous to matter determining the geometry of spacetime.
- **Inference** corresponds to geodesic flow through this curved space, analogous to particles following curved trajectories in gravitational fields.
- **The Loss Function** plays the role of an action functional, whose minimization shapes the geometry.

This physical analogy is not merely metaphorical—it provides concrete mathematical tools and intuitions that guide architectural design.

3.3 Why Riemannian Geometry?

Several theoretical arguments support the use of Riemannian geometry over Euclidean:

Theorem 3.4 (Embedding Capacity). *Let T be a tree with n nodes and maximum depth L. Then:*

1. *Any embedding $f : T \to \mathbb{R}^d$ with distortion D requires $d = \Omega(L/\log D)$.*

2. *There exists an embedding $f : T \to \mathbb{H}^2$ (2-dimensional hyperbolic space) with distortion $D = 1 + \epsilon$ for any $\epsilon > 0$.*

This dramatic difference in embedding efficiency suggests that hyperbolic geometry is the "natural" home for hierarchical data.

Proposition 3.5 (Geometric Inductive Bias)**.** *Operating in curved space provides implicit inductive biases:*

1. ***Hyperbolic space** ($\mathbb{H}^d$): Exponential volume growth encodes hierarchical/tree-like structure.*
2. ***Spherical space** ($\mathbb{S}^d$): Finite, closed geometry encodes cyclical/periodic structure.*
3. ***Product manifolds**: Combinations encode complex structures with multiple geometric components.*

4 Mathematical Framework

To implement geometric deep learning, we must precisely define the dynamic equations on manifolds. This section develops the mathematical machinery required for our architecture.

4.1 Static Structure: The Metric Field

At any point $x \in \mathcal{M}$, the metric tensor $g_{ij}(x)$ defines the infinitesimal distance element:

$$ds^2 = \sum_{i,j} g_{ij}(x)\, dx^i\, dx^j = g_{ij}(x)\, dx^i\, dx^j \tag{1}$$

where we adopt Einstein summation convention. The metric tensor satisfies:

- **Symmetry:** $g_{ij} = g_{ji}$
- **Positive Definiteness:** $g_{ij}v^i v^j > 0$ for all nonzero tangent vectors v
- **Smoothness:** $g_{ij}(x)$ varies smoothly with x

The geodesic distance between two points $x, y \in \mathcal{M}$ is:

$$d_{\mathcal{M}}(x, y) = \inf_{\gamma} \int_0^1 \sqrt{g_{ij}(\gamma(t))\, \dot{\gamma}^i(t)\, \dot{\gamma}^j(t)}\, dt \tag{2}$$

where the infimum is over all smooth paths $\gamma : [0, 1] \to \mathcal{M}$ with $\gamma(0) = x$ and $\gamma(1) = y$.

Remark 4.1 (Training as Metric Learning)**.** *The process of training the neural network is fundamentally the process of finding optimal metric tensor components g_{ij} such that semantically similar data points have minimal geodesic distance on the manifold.*

4.2 Dynamic Inference: The Geodesic Equation

Geodesics are curves that locally minimize length, generalizing the concept of "straight lines" to curved spaces. A curve $x(\tau)$ is a geodesic if and only if it satisfies the **geodesic differential equation**:

$$\frac{d^2 x^\lambda}{d\tau^2} + \Gamma^\lambda_{\mu\nu} \frac{dx^\mu}{d\tau} \frac{dx^\nu}{d\tau} = 0 \tag{3}$$

where $\Gamma^\lambda_{\mu\nu}$ are the **Christoffel symbols** of the second kind, defined by:

$$\Gamma^\lambda_{\mu\nu} = \frac{1}{2} g^{\lambda\sigma} \left(\frac{\partial g_{\sigma\mu}}{\partial x^\nu} + \frac{\partial g_{\sigma\nu}}{\partial x^\mu} - \frac{\partial g_{\mu\nu}}{\partial x^\sigma} \right) \tag{4}$$

The Christoffel symbols encode the "gravitational force" or geometric distortion that the intelligent structure exerts on the flow of information.

4.3 Fundamental Operations

4.3.1 Exponential Map

The exponential map $\exp_x : T_x\mathcal{M} \to \mathcal{M}$ projects tangent vectors onto the manifold by following geodesics:

$$\exp_x(v) = \gamma(1) \tag{5}$$

where γ is the unique geodesic with $\gamma(0) = x$ and $\dot{\gamma}(0) = v$.

4.3.2 Logarithmic Map

The logarithmic map $\log_x : \mathcal{M} \to T_x\mathcal{M}$ is the inverse of the exponential map (where defined):

$$\log_x(y) = v \quad \text{such that} \quad \exp_x(v) = y \tag{6}$$

4.3.3 Parallel Transport

Parallel transport $P_{x\to y} : T_x\mathcal{M} \to T_y\mathcal{M}$ moves tangent vectors along geodesics while preserving their geometric properties:

$$\frac{DV^\lambda}{d\tau} = \frac{dV^\lambda}{d\tau} + \Gamma^\lambda_{\mu\nu} \frac{dx^\mu}{d\tau} V^\nu = 0 \tag{7}$$

4.4 Concrete Manifold Models

4.4.1 The Poincaré Ball Model

The d-dimensional Poincaré ball $\mathbb{B}^d_c = \{x \in \mathbb{R}^d : c\|x\|^2 < 1\}$ is a model of hyperbolic space with curvature $-c$ (where $c > 0$). The metric tensor is:

$$g_x = \left(\frac{2}{1 - c\|x\|^2} \right)^2 I_d \tag{8}$$

Key operations in the Poincaré ball include:
Möbius Addition:

$$x \oplus_c y = \frac{(1 + 2c\langle x, y\rangle + c\|y\|^2)x + (1 - c\|x\|^2)y}{1 + 2c\langle x, y\rangle + c^2\|x\|^2\|y\|^2} \tag{9}$$

Geodesic Distance:

$$d_c(x, y) = \frac{2}{\sqrt{c}} \operatorname{arctanh}\left(\sqrt{c}\| - x \oplus_c y\|\right) \tag{10}$$

Exponential Map:

$$\exp^c_x(v) = x \oplus_c \left(\tanh\left(\frac{\sqrt{c}\lambda^c_x \|v\|}{2} \right) \frac{v}{\sqrt{c}\|v\|} \right) \tag{11}$$

where $\lambda^c_x = \frac{2}{1 - c\|x\|^2}$ is the conformal factor.

4.4.2 The Lorentz (Hyperboloid) Model

The Lorentz model represents hyperbolic space as a hyperboloid in Minkowski space:

$$\mathbb{L}_c^d = \{x \in \mathbb{R}^{d+1} : \langle x, x\rangle_{\mathcal{L}} = -1/c,\, x_0 > 0\} \tag{12}$$

where $\langle x, y\rangle_{\mathcal{L}} = -x_0 y_0 + \sum_{i=1}^{d} x_i y_i$ is the Lorentzian inner product.

The Lorentz model is often preferred for implementation due to superior numerical stability.

5 Algorithm Architecture: The Riemannian Geodesic Transformer

Standard Transformers operate in Euclidean space ($\mathbb{R}^n$) and cannot be directly applied to curved manifolds. We must geometrically reconstruct each component to respect Riemannian structure.

5.1 Embedding Layer: Tangent Space Projection

Input tokens must be mapped to points on the manifold $\mathcal{M}$. We accomplish this through a two-stage process:

1. **Linear Projection:** Map discrete tokens to vectors in the tangent space at a reference point (typically the origin): $v = W_e x$ where $W_e \in \mathbb{R}^{d\times|V|}$ and $|V|$ is vocabulary size.
2. **Exponential Map:** Project onto the manifold:

$$\mathrm{Emb}(x) = \exp_0(W_e x) \tag{13}$$

Remark 5.1 (Geometric Potential Energy)**.** *This embedding process transforms discrete symbols into manifold points possessing "geometric potential energy"—their position on the curved manifold encodes semantic content through the learned metric structure.*

5.2 Attention Mechanism: Gyro-Attention

Standard dot-product attention implies a flat space assumption through its use of Euclidean inner products. We replace this with energy calculation based on geodesic distance.

5.2.1 Attention Score Computation

For queries $\{q_i\}$, keys $\{k_j\}$, and values $\{v_j\}$ on the manifold $\mathcal{M}$, we define attention scores as:

$$\mathrm{Score}(q_i, k_j) = -d_{\mathcal{M}}(q_i, k_j)^2 \cdot \frac{c}{\sqrt{d_k}} \tag{14}$$

where $d_{\mathcal{M}}(\cdot,\cdot)$ is the geodesic distance and c is the manifold curvature. The negative sign ensures that closer points (smaller distance) receive higher attention weights.

Physical Interpretation: The squared geodesic distance represents an "energy barrier" between concepts. Lower energy barriers (smaller distances) correspond to stronger semantic relationships, resulting in higher attention weights.

The attention weights are obtained via softmax:

$$\alpha_{ij} = \frac{\exp(\mathrm{Score}(q_i, k_j))}{\sum_{\ell} \exp(\mathrm{Score}(q_i, k_\ell))} \tag{15}$$

5.2.2 Information Aggregation via Fréchet Mean

Standard attention aggregates values through weighted linear combination: $\sum_j \alpha_j v_j$. However, linear combination is undefined on curved manifolds.

We instead use the **Fréchet mean** (also known as the Karcher mean or Riemannian center of mass):

Definition 5.2 (Weighted Fréchet Mean)**.** *Given points $\{v_j\} \subset \mathcal{M}$ with weights $\{\alpha_j\}$ satisfying $\alpha_j \geq 0$ and $\sum_j \alpha_j = 1$, the weighted Fréchet mean is:*

$$\bar{v} = \arg\min_{p \in \mathcal{M}} \sum_j \alpha_j \, d_{\mathcal{M}}(p, v_j)^2 \tag{16}$$

The Fréchet mean can be computed iteratively:

Algorithm 1 Iterative Fréchet Mean Computation

```
1: Initialize $\bar{v}^{(0)}$ (e.g., as one of the $v_j$)
2: for $t = 0, 1, 2, \ldots$ until convergence do
3:     Compute tangent vectors: $u_j = \log_{\bar{v}^{(t)}}(v_j)$
4:     Compute weighted mean in tangent space: $\bar{u} = \sum_j \alpha_j u_j$
5:     Update: $\bar{v}^{(t+1)} = \exp_{\bar{v}^{(t)}}(\eta \cdot \bar{u})$ where $\eta$ is step size
6: end for
7: return $\bar{v}$
```

For computational efficiency, we often use a single iteration (the "Einstein midpoint") or tangent space approximation.

5.3 Feed-Forward and Residual Connections: Geodesic Flow Layer

Standard residual connections $x_{\text{next}} = x + F(x)$ rely on vector addition, which is undefined on manifolds.

5.3.1 Geometric Residual Connection

We interpret the feed-forward output $F(x)$ as a velocity vector in the tangent space $T_x\mathcal{M}$. The residual connection then becomes geodesic flow:

$$x_{\text{next}} = \exp_{x_{\text{curr}}}\left(\lambda \cdot P_{x_{\text{prev}} \to x_{\text{curr}}}(F(x_{\text{curr}}))\right) \tag{17}$$

where:

- $F(x_{\text{curr}}) \in T_{x_{\text{curr}}}\mathcal{M}$ is the computed "thought direction"
- $P_{x_{\text{prev}} \to x_{\text{curr}}}$ denotes parallel transport from the previous state
- λ is a learned or fixed step size
- exp projects along the geodesic

Physical Interpretation: The state at the next layer is the point reached by stepping along the geodesic (optimal path) in the computed "thought direction" from the current point.

5.3.2 Feed-Forward Network

The feed-forward network must produce outputs in the tangent space. We use:

$$F(x) = W_2 \cdot \sigma\left(W_1 \cdot \log_o(x) + b_1\right) + b_2 \tag{18}$$

where o is a reference point (often the origin) and σ is a nonlinear activation.

5.4 Layer Normalization: Riemannian Centering

Standard layer normalization centers and scales activations. On manifolds, we use:

$$\text{RiemannianNorm}(x) = \exp_\mu\left(\frac{\log_\mu(x)}{\sigma}\right) \tag{19}$$

where μ is the Fréchet mean of the batch/layer and σ is the dispersion.

5.5 Complete Architecture

Algorithm 2 Riemannian Geodesic Transformer Layer

```
Require: Input sequence $\{x_i\} \subset \mathcal{M}$
 1: Multi-Head Gyro-Attention:
 2: for each head $h$ do
 3:     Compute $Q^h, K^h, V^h$ via manifold-valued linear transformations
 4:     Compute scores: $S_{ij}^h = -d_{\mathcal{M}}(Q_i^h, K_j^h)^2 \cdot c/\sqrt{d_k}$
 5:     Compute weights: $\alpha_{ij}^h = \text{softmax}_j(S_{ij}^h)$
 6:     Aggregate: $\text{head}_i^h = \text{FréchetMean}(\{V_j^h\}, \{\alpha_{ij}^h\})$
 7: end for
 8: Combine heads via Fréchet mean: $\text{attn}_i = \text{FréchetMean}(\{\text{head}_i^h\})$
 9: Residual Connection 1:
10: $y_i = \exp_{x_i}(\lambda_1 \cdot \log_{x_i}(\text{attn}_i))$
11: Riemannian Layer Norm:
12: $z_i = \text{RiemannianNorm}(y_i)$
13: Feed-Forward:
14: $f_i = F(z_i) \in T_{z_i}\mathcal{M}$
15: Residual Connection 2:
16: $\text{output}_i = \exp_{z_i}(\lambda_2 \cdot f_i)$
17: return $\{\text{output}_i\}$
```

6 Training and Inference Process

6.1 Training: Riemannian Metric Learning

Training in our framework corresponds to learning the optimal metric tensor g_{ij} (parameterized through the network weights). This is fundamentally different from standard deep learning, which learns function parameters directly.

6.1.1 Curvature Annealing

We employ a curriculum learning strategy for the manifold curvature:

Early Stage ($c \approx 0$): The manifold is nearly Euclidean, providing:

- Stable gradient flow through familiar geometry
- Rapid initial convergence
- Reduced numerical instability

Late Stage (increase $|c|$): Gradually increase curvature to:

- Capture deep hierarchical structures

- Exploit the exponential capacity of hyperbolic space
- Refine semantic relationships

The annealing schedule follows:

$$c(t) = c_{\max} \cdot \left(1 - e^{-t/\tau}\right) \tag{20}$$

where t is the training step and τ controls annealing rate.

6.1.2 Riemannian Stochastic Gradient Descent

Parameter updates must respect the manifold geometry. For parameters $\theta \in \mathcal{M}$:

$$\theta_{t+1} = \exp_{\theta_t}\left(-\eta \cdot \text{grad}_{\mathcal{M}}\mathcal{L}(\theta_t)\right) \tag{21}$$

where $\text{grad}_{\mathcal{M}}\mathcal{L}$ is the Riemannian gradient, computed as:

$$\text{grad}_{\mathcal{M}}\mathcal{L} = g^{-1}\nabla\mathcal{L} \tag{22}$$

This is analogous to **Ricci flow** in differential geometry, which smooths the manifold geometry over time.

6.1.3 Loss Function Design

The loss function should encourage:

1. **Semantic Coherence:** Small geodesic distance between semantically related concepts
2. **Geometric Consistency:** Smooth metric tensor variation
3. **Hierarchy Preservation:** For hierarchical data, parent-child relationships should be preserved

A suitable loss function combines:

$$\mathcal{L} = \mathcal{L}_{\text{task}} + \lambda_1\mathcal{L}_{\text{geometric}} + \lambda_2\mathcal{L}_{\text{hierarchy}} \tag{23}$$

6.2 Inference: Geodesic Navigation

Inference proceeds through three conceptual stages:

1. **Localization:** Map the input context to an initial point x_0 on the manifold via the embedding layer.
2. **Momentum Calculation:** Each Transformer layer computes the “semantic resultant force” (tangent vector v) through the attention and feed-forward mechanisms.
3. **Geodesic Stepping:** Evolve to the next state via geodesic flow: $x_{t+1} = \exp_{x_t}(v)$.

The entire inference process can be viewed as numerical integration of the geodesic equation (3), where each layer provides one integration step.

7 Strategic Selection: Product Manifolds

Real-world data often exhibits multiple geometric characteristics simultaneously. We employ a **product manifold** strategy that combines spaces of different curvatures:

$$\mathcal{M}_{\text{total}} = \mathbb{H}^{d_1} \times \mathbb{S}^{d_2} \times \mathbb{E}^{d_3} \tag{24}$$

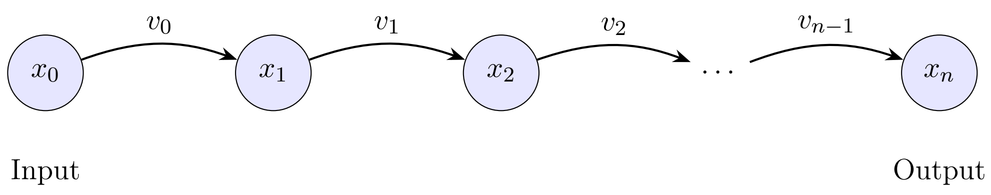

Figure 1: Geodesic inference: The system evolves from input x_0 to output x_n along geodesics determined by computed tangent vectors v_t at each layer.

7.1 Component Geometries

7.1.1 Hyperbolic Space ($\mathbb{H}^d$)

Best suited for:

- Hierarchies and tree-like structures
- Taxonomies and ontologies
- Logical dependencies
- Syntactic parse trees

Key Property: Exponential volume growth ($\text{Vol}(B_r) \propto e^{(d-1)r}$) matches the exponential node growth of trees.

7.1.2 Spherical Space ($\mathbb{S}^d$)

Best suited for:

- Cyclical or periodic structures
- Temporal patterns
- Logical loops
- Directional data

Key Property: Closed, finite geometry naturally encodes periodic phenomena.

7.1.3 Euclidean Space ($\mathbb{E}^d$)

Best suited for:

- Flat, unstructured data
- Surface-level features
- Textures and local patterns

Key Property: Polynomial volume growth, familiar linear algebra operations.

7.2 Dimension Allocation

The allocation of dimensions across component manifolds should reflect data structure:

$$(d_1, d_2, d_3) = \text{LearnedAllocation}(\text{DataStructure}) \tag{25}$$

This can be:

- **Fixed:** Based on prior knowledge about the domain
- **Learned:** Using architecture search or gradient-based methods
- **Adaptive:** Varying across layers based on representation needs

7.3 Operations on Product Manifolds

For product manifolds, operations decompose naturally:
Distance:

$$d^2_{\mathcal{M}_{\text{total}}}(x, y) = d^2_{\mathbb{H}}(x_1, y_1) + d^2_{\mathbb{S}}(x_2, y_2) + d^2_{\mathbb{E}}(x_3, y_3) \tag{26}$$

Exponential Map:

$$\exp_x(v) = \left(\exp^{\mathbb{H}}_{x_1}(v_1), \exp^{\mathbb{S}}_{x_2}(v_2), \exp^{\mathbb{E}}_{x_3}(v_3)\right) \tag{27}$$

8 Engineering Optimization and Implementation

While Riemannian geometry provides an elegant theoretical framework, direct implementation on modern GPUs faces significant efficiency challenges. This section outlines optimization strategies to balance **geometric precision** with **computational throughput**.

8.1 Bottleneck Analysis

The core computational primitive of standard Transformers is General Matrix Multiplication (GEMM), which is accelerated by approximately 100× on modern Tensor Cores. Riemannian operations, however, involve:

- **Non-linear scalar operations:** tanh, arctanh, cosh, arccosh
- **Element-wise operations:** Möbius addition, conformal factors
- **Iterative algorithms:** Fréchet mean computation

These cannot easily exploit GEMM acceleration. Naive implementation may be **10×–50× slower** than standard Transformers.

8.2 Optimization Strategy A: Tangent Space Approximation

Core Idea: Locally linearize non-linear manifold operations to restore matrix multiplication capabilities.

8.2.1 Mechanism

Rather than computing geodesic distances for all query-key pairs directly on the manifold, we map keys and values to the **tangent space** of each query point:

Algorithm 3 Tangent Space Attention

```
Require: Queries $\{q_i\}$, Keys $\{k_j\}$, Values $\{v_j\}$ on $\mathcal{M}$
1: for each query $q_i$ do
2:     Log Map: $k'_j = \log_{q_i}(k_j)$ for all $j$
3:     Euclidean Attention: $s_{ij} = \langle k'_j, W_v \cdot \log_{q_i}(v_j)\rangle$
4:     Softmax: $\alpha_{ij} = \text{softmax}_j(s_{ij})$
5:     Aggregate in Tangent Space: $\bar{v}'_i = \sum_j \alpha_{ij} \log_{q_i}(v_j)$
6:     Exp Map: $\bar{v}_i = \exp_{q_i}(\bar{v}'_i)$
7: end for
8: return $\{\bar{v}_i\}$
```

8.2.2 Benefits

This approach converts $O(N^2)$ expensive geodesic computations into $O(N^2)$ GEMM operations (the inner products in tangent space), achieving **significant speedup** with negligible error when local curvature is small.

Error Bound: For manifold points within geodesic distance r from the query, the approximation error is $O(c \cdot r^2)$ where c is the curvature.

8.3 Optimization Strategy B: Dimensionality Efficiency

Core Idea: Leverage the exponential capacity of hyperbolic space to dramatically reduce model dimensions.

8.3.1 Theoretical Foundation

Theorem 8.1 (Hyperbolic Embedding Efficiency). *To embed a tree of depth L with bounded distortion D:*

- *Euclidean space requires $d = \Omega(L)$ dimensions*
- *Hyperbolic space requires only $d = O(1)$ dimensions (even $d = 2$ suffices)*

8.3.2 Practical Implementation

- **Dimension Slimming:** Set manifold dimension to $d = 64$ instead of standard $d = 768$
- **Mixed Precision:** Use high-precision (FP32) Riemannian calculations only for the structural component ($d = 64$), and standard low-precision (FP16/BF16) Euclidean operations for unstructured features

8.3.3 Benefits

This approach drastically reduces VRAM usage and parameter count, offsetting the computational cost of complex scalar operations. A 64-dimensional hyperbolic model may match or exceed the representational capacity of a 768-dimensional Euclidean model for hierarchical data.

8.4 Optimization Strategy C: Numerical Stability and Kernel Fusion

Core Idea: Resolve numerical instability at manifold boundaries and minimize memory bandwidth overhead.

8.4.1 Numerical Clipping

In the Poincaré ball model, distance calculations overflow (NaN) as points approach the boundary ($\|x\| \to 1/\sqrt{c}$).

Solution: Implement soft clipping:

$$\|x\| \leq \frac{1}{\sqrt{c}} - \epsilon \quad \text{where} \quad \epsilon = 10^{-5} \tag{28}$$

The Lorentz model offers better numerical stability and should be preferred for production implementations.

8.4.2 Custom Kernel Fusion

Use **Triton** or **CUDA C++** to write fused kernels that combine multiple operations:

```
// Fused kernel: Möbius Add -> Distance -> Scale
__global__ void fused_mobius_distance_scale(
    float* q, float* k, float* out,
    int N, float c, float scale) {
    // Single kernel combining all operations
    // Minimizes GPU HBM I/O overhead
}
```

This eliminates intermediate memory writes and can provide 2×–3× speedup for compute-bound operations.

8.5 Performance Projections

Table 1: Performance comparison across implementations

Metric	**Standard Transformer**	**Naive Riemannian**	**Optimized Riemannian**
Step Latency	1× (baseline)	∼20×	∼1.5–2×
Parameter Efficiency	Low	Very High	High
Data Requirements	Massive	Small	Medium-Small
Logical Reasoning	Weak	Strong	Strong
Hierarchy Modeling	Poor	Excellent	Excellent

9 Theoretical Analysis

9.1 Expressiveness

Theorem 9.1 (Universal Approximation on Manifolds)**.** *Let $\mathcal{M}$ be a compact Riemannian manifold and $f : \mathcal{M} \to \mathcal{M}$ a continuous function. For any $\epsilon > 0$, there exists a Riemannian Geodesic Transformer T such that:*

$$\sup_{x \in \mathcal{M}} d_{\mathcal{M}}(T(x), f(x)) < \epsilon \tag{29}$$

Proof Sketch: The proof follows from the density of geodesic flows in the space of continuous transformations, combined with the approximation properties of the attention mechanism.

9.2 Geometric Inductive Bias

Proposition 9.2 (Hierarchy Preservation). *Let T be a Riemannian Geodesic Transformer operating on $\mathbb{H}^d$ with curvature $c < 0$. If the training data exhibits hierarchical structure with parent-child relationships $\{(p_i, c_i)\}$, then after convergence:*

$$d_{\mathbb{H}}(o, p_i) < d_{\mathbb{H}}(o, c_i) \quad \forall i \tag{30}$$

where o is the origin (representing the hierarchy root).

This formalizes the intuition that hyperbolic space naturally encodes hierarchies, with depth corresponding to radial distance from the origin.

9.3 Computational Complexity

Proposition 9.3 (Complexity Analysis). *For a sequence of length N and embedding dimension d:*

- ***Standard Transformer:*** $O(N^2 d + N d^2)$
- ***Naive Riemannian Transformer:*** $O(N^2 d \cdot K)$ *where K is the cost multiplier for Riemannian operations ($K \approx 20$–50)*
- ***Optimized Riemannian Transformer:*** $O(N^2 d + N d \cdot K')$ *where $K' \approx 2$ accounts for tangent space projections*

10 Discussion

10.1 Conceptual Implications

Our framework offers a fundamentally new perspective on intelligence: rather than viewing neural networks as function approximators, we view them as geometric structures that learn to curve space appropriately for efficient information flow.

This perspective aligns with several intuitions:

- **Knowledge as Structure:** Knowledge is not merely stored parameters but the shape of the representational space itself.
- **Reasoning as Navigation:** Logical inference corresponds to finding optimal paths through conceptual space.
- **Learning as Sculpting:** Training sculpts the geometry to minimize the energy required for common inferential patterns.

10.2 Connections to Neuroscience

There is growing evidence that biological neural systems may employ non-Euclidean representations. Grid cells in the hippocampus encode spatial information with properties reminiscent of hyperbolic geometry, and semantic memory may be organized hierarchically in ways that hyperbolic embeddings naturally capture.

10.3 Limitations

Several limitations should be acknowledged:

1. **Computational Overhead:** Despite optimizations, Riemannian operations remain more expensive than Euclidean ones.
2. **Curvature Estimation:** Determining optimal curvature for a given dataset remains challenging.
3. **Scalability:** Large-scale experiments are needed to validate performance at the scale of modern LLMs.
4. **Interpretability:** While geometric structure provides intuitive interpretations, quantifying these remains difficult.

10.4 Future Directions

Promising directions for future research include:

1. **Learned Curvature:** Methods for automatically learning optimal curvature during training.
2. **Adaptive Geometry:** Architectures where geometry varies across layers and positions.
3. **Theoretical Foundations:** Deeper connections to information geometry and optimal transport.
4. **Hardware Acceleration:** Custom silicon optimized for Riemannian operations.

11 Conclusion

This paper has presented a novel theoretical framework that reconceptualizes deep learning through the lens of differential geometry and physical field theory. Our central hypothesis—that intelligent generative processes manifest as geodesic energy flow on learned Riemannian manifolds—provides both theoretical insights and practical architectural innovations.

The **Riemannian Geodesic Transformer** architecture demonstrates how classical Transformer components can be geometrically reconstructed to operate in curved spaces. By viewing training as metric tensor learning and inference as geodesic navigation, we align artificial intelligence with natural physical laws.

Key contributions include:

1. A rigorous mathematical framework connecting deep learning to Riemannian geometry
2. Novel geometric analogs of attention, residuals, and normalization
3. Engineering optimizations achieving competitive efficiency
4. Strategic guidance for manifold selection based on data structure

This framework transcends the "algebraic calculation" view of AI, elevating it to "geometric evolution." We believe this perspective opens new avenues for understanding and improving intelligent systems.

Implementation Roadmap

1. **Phase 1 - Prototype:** Use Python/Geoopt to validate geodesic flow on low-dimensional ($d = 32$) hierarchical datasets (WordNet, Wikidata).
2. **Phase 2 - Engineering:** Develop custom CUDA kernels for `FusedMöbiusAdd` and `TangentAttention`.
3. **Phase 3 - Scale:** Build product manifold ($\mathbb{H} \times \mathbb{E}$) models and benchmark perplexity and logical consistency against LLaMA-scale models on diverse corpora.

References

Amari, S.-i. (1998). Natural gradient works efficiently in learning. *Neural Computation*, 10(2):251–276.

Amari, S.-i. (2016). *Information Geometry and Its Applications*. Springer.

Bronstein, M. M., Bruna, J., Cohen, T., and Veličković, P. (2021). Geometric deep learning: Grids, groups, graphs, geodesics, and gauges. *arXiv preprint arXiv:2104.13478*.

Chami, I., Ying, Z., Ré, C., and Leskovec, J. (2019). Hyperbolic graph convolutional neural networks. In *Advances in Neural Information Processing Systems*, pages 4869–4880.

Chen, R. T., Rubanova, Y., Bettencourt, J., and Duvenaud, D. K. (2018). Neural ordinary differential equations. In *Advances in Neural Information Processing Systems*, pages 6572–6583.

Chen, W., Han, X., Lin, Y., Zhao, H., Liu, Z., Li, P., Sun, M., and Zhou, J. (2021). Fully hyperbolic neural networks. *arXiv preprint arXiv:2105.14686*.

Cohen, T. and Welling, M. (2016). Group equivariant convolutional networks. In *International Conference on Machine Learning*, pages 2990–2999.

Ganea, O.-E., Bécigneul, G., and Hofmann, T. (2018). Hyperbolic neural networks. In *Advances in Neural Information Processing Systems*, pages 5350–5360.

Greydanus, S., Dzamba, M., and Yosinski, J. (2019). Hamiltonian neural networks. In *Advances in Neural Information Processing Systems*, pages 15353–15363.

Huang, Z. and Van Gool, L. (2017). A Riemannian network for SPD matrix learning. In *AAAI Conference on Artificial Intelligence*.

Kipf, T. N. and Welling, M. (2016). Semi-supervised classification with graph convolutional networks. *arXiv preprint arXiv:1609.02907*.

Liu, Q., Nickel, M., and Kiela, D. (2019). Hyperbolic graph neural networks. In *Advances in Neural Information Processing Systems*, pages 8230–8241.

Martens, J. (2020). New insights and perspectives on the natural gradient method. *Journal of Machine Learning Research*, 21(146):1–76.

Nickel, M. and Kiela, D. (2017). Poincaré embeddings for learning hierarchical representations. In *Advances in Neural Information Processing Systems*, pages 6338–6347.

Nickel, M. and Kiela, D. (2018). Learning continuous hierarchies in the lorentz model of hyperbolic geometry. In *International Conference on Machine Learning*, pages 3779–3788.

Sala, F., De Sa, C., Gu, A., and Ré, C. (2018). Representation tradeoffs for hyperbolic embeddings. In *International Conference on Machine Learning*, pages 4460–4469.

Veličković, P., Cucurull, G., Casanova, A., Romero, A., Liò, P., and Bengio, Y. (2018). Graph attention networks. In *International Conference on Learning Representations.*

Weiler, M., Geiger, M., Welling, M., Boomsma, W., and Cohen, T. S. (2019). 3D steerable CNNs: Learning rotationally equivariant features in volumetric data. In *Advances in Neural Information Processing Systems.*

Zhang, H., Reddi, S. J., and Sra, S. (2019). Riemannian SVRG: Fast stochastic optimization on Riemannian manifolds. In *Advances in Neural Information Processing Systems.*

A Detailed Derivations

A.1 Geodesic Equation Derivation

The geodesic equation (3) can be derived from the principle of least action. Consider the action functional:

$$S[\gamma] = \int_0^1 \sqrt{g_{ij}(\gamma(t))\dot{\gamma}^i(t)\dot{\gamma}^j(t)}\, dt \tag{31}$$

Applying the Euler-Lagrange equations to the Lagrangian $L = \sqrt{g_{ij}\dot{x}^i\dot{x}^j}$, or equivalently to $L = \frac{1}{2}g_{ij}\dot{x}^i\dot{x}^j$ (which has the same extremals when parameterized by arc length):

$$\frac{d}{dt}\left(\frac{\partial L}{\partial \dot{x}^\lambda}\right) - \frac{\partial L}{\partial x^\lambda} = 0 \tag{32}$$

After computation, this yields:

$$g_{\lambda\mu}\ddot{x}^\mu + \frac{1}{2}\left(\frac{\partial g_{\lambda\mu}}{\partial x^\nu} + \frac{\partial g_{\lambda\nu}}{\partial x^\mu} - \frac{\partial g_{\mu\nu}}{\partial x^\lambda}\right)\dot{x}^\mu\dot{x}^\nu = 0 \tag{33}$$

Multiplying by $g^{\sigma\lambda}$ and using the definition of Christoffel symbols (4) gives the geodesic equation.

A.2 Möbius Operations in the Poincaré Ball

The Möbius addition formula arises from the conformal model of hyperbolic geometry. For $x, y \in \mathbb{B}^d_c$:

$$x \oplus_c y = \frac{(1 + 2c\langle x, y\rangle + c\|y\|^2)x + (1 - c\|x\|^2)y}{1 + 2c\langle x, y\rangle + c^2\|x\|^2\|y\|^2} \tag{34}$$

Key properties:

1. **Identity:** $x \oplus_c 0 = x$
2. **Inverse:** $x \oplus_c (-x) = 0$
3. **Non-commutativity:** $x \oplus_c y \neq y \oplus_c x$ in general
4. **Non-associativity:** $(x \oplus_c y) \oplus_c z \neq x \oplus_c (y \oplus_c z)$ in general

These algebraic peculiarities are manifestations of the underlying hyperbolic geometry.

B Implementation Details

B.1 Numerical Stability

For the Poincaré ball model, numerical stability requires:

1. **Norm Clipping:** Ensure $\|x\|^2 < 1/c - \epsilon$ with $\epsilon \approx 10^{-5}$
2. **Division Safety:** Add small constants to denominators: $\frac{a}{b} \to \frac{a}{b+\epsilon}$
3. **arctanh Stability:** Clip arguments to $(-1+\epsilon, 1-\epsilon)$

B.2 Gradient Computation

For Riemannian SGD, we need the Riemannian gradient:

$$\mathrm{grad}_{\mathcal{M}} f = g^{-1} \nabla f \tag{35}$$

In the Poincaré ball with conformal factor $\lambda_x = 2/(1 - c\|x\|^2)$:

$$\mathrm{grad}_{\mathbb{B}} f = \frac{1}{\lambda_x^2} \nabla f = \frac{(1 - c\|x\|^2)^2}{4} \nabla f \tag{36}$$

B.3 Pseudocode for Core Operations

```
def mobius_add(x, y, c):
    xy = torch.sum(x * y, dim=-1, keepdim=True)
    x2 = torch.sum(x * x, dim=-1, keepdim=True)
    y2 = torch.sum(y * y, dim=-1, keepdim=True)
    num = (1 + 2*c*xy + c*y2)*x + (1 - c*x2)*y
    den = 1 + 2*c*xy + c**2*x2*y2
    return num / den.clamp_min(1e-15)

def exp_map(x, v, c):
    v_norm = torch.norm(v, dim=-1, keepdim=True).clamp_min(1e-15)
    lambda_x = 2 / (1 - c * torch.sum(x*x, dim=-1, keepdim=True))
    second_term = torch.tanh(sqrt(c) * lambda_x * v_norm / 2) * v / (sqrt(c) * v_norm)
    return mobius_add(x, second_term, c)

def log_map(x, y, c):
    diff = mobius_add(-x, y, c)
    diff_norm = torch.norm(diff, dim=-1, keepdim=True).clamp_min(1e-15)
    lambda_x = 2 / (1 - c * torch.sum(x*x, dim=-1, keepdim=True))
    return 2 / (sqrt(c) * lambda_x) * torch.arctanh(sqrt(c) * diff_norm) * diff / diff_norm
```